CHARACTERIZATION OF CELLULOSE NANOFIBRILS-PNIPAAm COMPOSITE HYDROGELS AT DIFFERENT CARBOXYL CONTENTS

NANANG MASRUCHIN, *BYUNG-DAE PARK** and VALERIO CAUSIN***

[*]Department Wood and Paper Sciences, Kyungpook National University, Daegu 41566, Republic of Korea
[**]Institute of Agricultural Science and Technology, Kyungpook National University, Daegu, 41566, Republic of Korea
[***]Department of Chemical Sciences, University of Padova, via Marzolo 1, 35131, Padova, Italy
✉ *Corresponding author: Byung-Dae Park, byung-dae@knu.ac.kr*

Received October 18, 2016

As part of the research on fabricating functional materials based on cellulose, this study characterized composite hydrogels prepared by combining cellulose nanofibrils (CNF) from 2,2,6,6-tetramethylpiperidinyl-1-oxyl(TEMPO)-mediated oxidation with poly(N-isopropylacrylamide) (PNIPAAm) *via in situ* polymerization above the lower critical solution temperature. We manipulated the surface carboxylate content level of CNFs by adjusting the amount of sodium hypochloride (NaClO) used as oxidant for the reaction to understand the effects of the carboxylate content on the characteristics of the CNF/PNIPAAm composite hydrogels. As expected, the CNF surface charge increased with an increase in the oxidant amount, which resulted in greater transparency owing to a better CNF dispersion in the polymer suspension. The surface charge level of CNF also influenced the compression strength of CNF/PNIPAAm hydrogels, which was supported by the rheological behavior of CNF. Namely, a lower surface charge level of CNF produced tight interconnections between the fibrils due to an entanglement of the remaining un-converted hydroxyl groups *via* hydrogen bonds within fibrillated CNFs. Meanwhile, at a higher surface charge level, the finer dispersed CNF at higher electrostatic repulsion slightly decreased fibril to fibril interactions. Fourier transform infrared (FTIR) spectra and differential scanning calorimetry (DSC) results indicated that the CNFs were physically bonded onto PNIPAAm in the hydrogels. These results showed that the surface charge level of the CNF had a great impact on the characteristics of the CNF/PNIPAAm hydrogels, indicating that the selection of a proper level of CNF surface charge and polymerization temperature would be important for developing temperature-responsive hydrogels.

Keywords: cellulose nanofibrils, TEMPO-oxidation, surface carboxyl charge level, PNIPAAm, hydrogel

INTRODUCTION

Cellulose nanofibrils (CNF) obtained by 2,2,6,6-tetramethylpiperidinyl-1-oxyl (TEMPO)-mediated oxidation provide CNFs with a surface charge, which can be used for the development of functional materials based on cellulose. In recent years, there have been a wide range of applications of the CNFs isolated by the TEMPO-mediated oxidation, *e.g*., as barrier films with low oxygen permeability,[1] papers with improved strength,[2] nanocomposites,[3] high-efficiency nanoporous filters for particulate air (HEPA),[4] nanoparticle deposition substrates,[5,6] native cellulose hydrogels,[7,8] and composite hydrogels.[9,10] These applications of CNFs obtained by TEMPO oxidation are based on the use of the aldehyde and/or carboxylate group on the CNF surface. The presence of the carboxylate group creates a negative charge on the surface of CNFs, which reduces the energy consumption for the isolation of CNFs, owing to their repulsive force in the suspension.[11,12] Tejado *et al.*[13] reported that CNFs were isolated by introducing carboxyl groups at C2 and C3 on the cellulose through periodate, followed by chlorite oxidation in the absence of mechanical energy if the degree of oxidation was sufficiently high. Their results indicated that the presence of negative surface charge as an internal force was tremendously effective for the defibrillation of cellulose. In the

case of the cellulose TEMPO-mediated oxidation system, several methods have been proposed to manipulate the carboxyl content of oxidized celluloses, such as adding different amounts of NaClO,[8,14] assisting ultrasonic treatment during the reaction,[15] conducting the reaction in a borax buffer solution,[16] or pre-treating the cellulose using formic acid prior to TEMPO-oxidation.[17] In addition, the presence of the sodium carboxylate group (-COO^-Na^+) on the CNF improves the hydrophilicity and can act as a reinforcing agent for poly(N-isopropylacrylamide) (PNIPAAm) hydrogels at the same time.[9,10,18]

PNIPAAm is a typical thermosensitive polymer that has been mainly exploited for its low critical solution temperature (LCST), which is approximately 32 °C, close to the human body temperature.[19] When the temperature of the environment rose above the LCST, the balance between the hydrophilic groups(-CONH-) and the hydrophobic groups(-$CH(CH)_3$-) in the polymer chains was interrupted, leading to the dominance of hydrophobic moieties.[20] This change is characterized by a dramatic shrinkage in the volume and release of water. The exploitation of this unique characteristic has been proposed for the development of bio-sensing[21] and thermosensitive drug delivery systems.[22]

Further, the carboxyl groups of CNFs produced by TEMPO oxidation in PNIPAAm have been widely used not only to improve the swelling properties of hydrogels, but also to produce temperature and pH responsive hydrogels for drug release applications, such as carboxyl group (COOH) from pullulan materials[19] and hemicelluloses.[23] There are a few reports on the use of carboxylated CNF (Cha *et al*.,[9] Wei *et al.*[10]). Both studies showed that a larger CNF loading resulted in an improvement of the mechanical strength, swelling properties, and pH responsiveness of CNF/PNIPAAm.[9] However, in fact, for obtaining the "on-off" switchable properties of hydrogels, a fast reswelling and deswelling of the hydrogel in response to temperature changes is required. Therefore, a higher CNF content will reduce the thermoresponsiveness of the PNIPAAm hydrogel. Here, we report having produced CNF/PNIPAAm hydrogels at different surface charge levels and a lower CNF loading.

A recent study by Wei *et al*.[18] reported the effect of the surface charge content on the morphologies and properties of PNIPAAm-based composite hydrogels prepared at a temperature below LCST. The behavior of the PNIPAAm-based hydrogel synthesized with 5% CNF displayed a slow response to external temperature, because the formation of a dense skin layer (bubbles) weakened and destroyed the hydrogen bonds as the temperature increased. This impermeable skin layer prevented water from diffusing out, which further limited the application of PNIPAAm, in particular, to adsorption-desorption, sensing and drug release.[20,24-26] Therefore, this study attempted to employ *in situ* free radical polymerization for producing temperature responsive CNF/ PNIPAAm composite hydrogels at different carboxyl contents of CNFs by adding different amounts of NaClO as oxidant for TEMPO-mediated oxidation of cellulose[12,14] and above the LCST (70°C). First, we investigated the rheological behavior of CNF suspensions at different levels of NaClO and then the effects of the carboxyl content on the CNF/PNIPAAm composite hydrogels by characterizing morphology, compressive strength, microstructure, LCST, swelling ratio, and temperature responsive properties. We expected to obtain fundamental characteristics of the CNF/PNIPAAm composite hydrogels as temperature and pH responsive functional materials.

EXPERIMENTAL

Materials

The raw cellulose materials used in this study were obtained from dried hardwood bleached kraft pulp (HWBKP) from a pulp mill in Korea, and were stored in a humidity chamber at 25°C before use. Chemical reagents, such as TEMPO, sodium bromide (NaBr), sodium hypochlorite (NaClO) solution, N-isopropyl acrylamide (NIPAAm), *N,N'*-methylenebis acrylamide (MBA), and ammonium persulfate (APS), were purchased from Sigma-Aldrich. Purified water was obtained by reverse osmosis using UpureROtech, Korea, with a conductivity of about 6 μS/cm.

Production of cellulose nanofibrils

Different concentrations of carboxyl on the surface of CNF were obtained by adding different amounts of NaClO, such as 4, 10, and 15 mL, for the TEMPO-oxidation reaction. Details of the production of CNF have been reported elsewhere.[27] In brief, 2 g of HWBKP was diluted in a water suspension with 0.025 g of TEMPO and 0.25 g NaBr. After all the reactants were diluted well, a pre-determined amount of NaClO was added dropwise into the reaction to keep the pH below 10 during the oxidation. Finally, the pH of the

TEMPO oxidation reaction was kept at 10.5 at 23 °C, and was monitored using a pH-meter by the addition of 0.5 N NaOH. The reaction was stopped after the pH reached a constant level. Prior to neutralizing to pH 7 by adding HCl, ethanol (~5 mL) was added to terminate the reaction. The TEMPO-oxidized pulp slurry was filtered and washed several times. CNF was isolated by subjecting the oxidized pulp to ultrasonication for 40 min using a Sonomasher (power 30%, frequency 20320 Hz) with a probe tip diameter of 1 cm. Further, the CNF was obtained from the supernatant and the unfibrillated fibers were separated in the sediment after centrifugation. The carboxyl content of CNF was measured using conductometric titration.[14]

Composite hydrogel preparation

Pure PNIPAAm and CNF-PNIPAAm composite hydrogels were synthesized *via in situ* polymerization in aqueous solution. One gram of NIPAAm, 3 wt% monomer of MBA, and 0.3wt% CNF solution were dissolved in 5 mL distilled water using a mini shaker. Bubbles were removed by using vacuum for 30 min. The mixture of monomer, crosslinker, and CNF was heated up to 70°C. After that, the initiator (APS) and 1wt% of monomer were dissolved and added dropwise into the mixture. Polymerization was conducted for 1 h. At the end, the prepared hydrogels were purified by immersing and rinsing several times using distilled water.

Characterization

Frequency sweep test (FST) and compression strength

The frequency sweep test and compression strength measurement were conducted using a dynamic rheometer (HAAKE MARS, Modulated Advanced Rheometer System, Germany). For the rheological measurements, a 60 mm diameter cone and a 35 mm diameter plate apparatus were used for the measurement of 0.3% w/w CNF suspension and of the composite hydrogel, respectively. A steady shear test was performed between 0.1 and 100 rad/s. The strain rate was determined to be in the linear viscoelastic regime and was 0.01%. In addition, for the compression strength, samples with 2 cm thickness were compressed using the plate setup. The experiments were repeated twice at 25 °C for each sample.

Transparency

In order to characterize the transparency of CNFs with different surface charge levels, the light transmittance of CNF suspensions was measured using a UV–VIS spectrophotometer (Optizen 3220UV, Mecasys Co., Ltd., Daejeon, Korea). The concentration of the CNF suspension was controlled at 0.3% (w/v). Data were collected over the wavelength range of 200 to 1000 nm.

ATR-FTIR analysis

Freeze-dried hydrogels were analyzed using attenuated total reflectance-Fourier transform infrared (ATR-FTIR) spectroscopy (ALPHA-P model, Bruker Optics, Germany). The absorption was measured over the range of 4000-400 cm^{-1}. In order to enhance the signal-to-noise ratio, an average value of 25 scans was obtained for each sample.

Different scanning calorimetry (DSC)

The LCST of the hydrogels was determined by DSC (Q2000, TA Instruments, USA). The hydrogel sample was allowed to swell in distilled water at room temperature until it reached an equilibrium swelling state. The sample surface was wiped with filter paper to remove free water. Then, about 5 mg of the swollen sample was placed in an aluminum pan. The DSC measurement was performed on swollen samples from 10 to 50°C at a rate of 5 °C/min to measure the LCST of the hydrogels.

Field emission scanning electron microscopy (FE-SEM)

Microscopic observation of the internal structure of the hydrogels was performed using FE-SEM (S-4800, Hitachi, Japan). The hydrogel samples were immersed in liquid nitrogen and freeze dried. The images of the fracture surface of the freeze-dried samples were obtained at an acceleration voltage of 5.0 kV. Prior to the observation, the samples were mounted on the specimen stubs, using carbon adhesive tape, and coated with osmic acid (OsO_4) by a VD HPC-ISW osmium coater (Tokyo, Japan).

Swelling behavior

Vacuum dried hydrogels were placed in a 50mL beaker, and then 30 mL of distilled water was added. The swollen hydrogel was filtered by a sieve after a pre-determined time interval, and the water absorption at a given swelling time was determined from the weight change before and after the swelling. The swelling ratio (SR) was calculated as follows:

$$SR = \frac{(W_t - W_d)}{W_d} \quad (1)$$

Where W_t and W_d represent the same quantities as in the water retention calculation.

Water retention

The hydrogel was first immersed at 20 °C until the equilibrium state was reached, and then transferred to a 50 °C distilled water bath. The weight of the hydrogel was monitored by removing the free water from the surface of the hydrogel with filter paper at predetermined time. The water retention was defined as follows:

$$WR\ (\%) = \frac{(W_t - W_d)}{W_s} x100 \quad (2)$$

Where W_t is the weight of wet hydrogel at time t; and W_s and W_d represent the weight of swollen (20 °C) and dry hydrogels, respectively.

RESULTS AND DISCUSSION

Characterization of CNFs

In this study, different levels of the carboxyl content (from 1.1 to 1.9 mmol/g) on the surface of CNF were obtained, and the characterization of these CNFs was done as presented in Figures 1, 2 and 3. Figure 1 displays the effect of NaClO addition to (a) the carboxyl content on the surface of CNFs, (b) FT-IR spectra, and (c) the quantitation of the carboxyl content based on the analysis of the FT-IR spectra. As expected, the carboxyl content increased with an increase in the amount of added NaClO (Fig. 1a), and the yield of CNF also increased by adding more NaClO into the reaction. This could be due to an increase in the degree of oxidation of cellulose by a greater amount of the oxidant.[28] Hence, subsequent oxidation reactions were done at lower levels of NaClO in order to obtain the same amount of the CNF stock suspension. At higher NaClO level, many primary hydroxyl groups were converted to aldehyde and further into carboxylate groups, which made the reaction last for a longer time, compared to that at lower NaClO content.[14]

Similar patterns of FT-IR spectra were observed in all CNF samples obtained by TEMPO-mediated oxidation, except the control sample (Fig. 1b). The broadened absorption band around 3000-3650 cm^{-1}, corresponding to the –OH stretching, was observed in all the samples. Further, the sharp peak at 897 cm^{-1} was attributed to the vibration and the ring frequency vibration of the C1 group, which is the characteristic absorption peak of the β-glycosidic bond.[29] An increased intensity in the peak observed from cellulose after oxidation indicated that the non-cellulosic compounds were diluted and removed from the cellulose after processing. In addition, the presence of carboxylate groups was detected by the very strong peak around 1605 and from 1413 to 1310 cm^{-1}, which was attributed to the anti-symmetric and symmetric stretching band of the COO^{-} group in carboxylic acid salts, respectively (Fig. 1b). These peaks did not appear on the HWBKP used as the raw cellulose material (Fig. 1b). In order to quantify the carboxyl content of CNF using the FT-IR spectra, we selected two absorption peaks of the FT-IR spectra: the absorption of the peak around 1033 cm^{-1} assigned to the -CO stretching of the carbonyl group was used as a reference to calculate the ratio of the absorption of the carboxylate group (A_{1607}) to that of the carbonyl group (A_{1033}) from ATR-FTIR analysis, because the absorption of the-CO stretching remained unchanged during the reaction.[30] These results confirm that the carboxyl group ratio increased by increasing the amount of NaClO added to the reaction. This result also agrees with the conductometric titration measurement (Fig. 1a).

Figure 2 shows the effects of the CNF surface charge on their rheological behaviors, such as the shear viscosity, shear stress, storage modulus (G′), and loss modulus (G″) of the CNF suspension. As the carboxyl content increased upon increasing the amount of NaClO, both the shear viscosity and shear stress of the CNF suspension decreased (Fig. 2a, b), which could be due to higher electrostatic repulsion and osmotic effect (anionic charge) of the CNFs in the suspension. An increased repulsive force in the suspension resulted in a shear thinning behavior loss of the suspension with the amount of NaClO in the order 4 mL < 10 mL <15 mL. This indicated the formation of fine nanofibrils as the amount of oxidant increased. Both G′ and G″ become more dependent on the angular frequency (Fig. 2c, d), which could be due to the oxidation of cellulose using the TEMPO/NaBr/NaClO system, leading to the depolymerization of cellulose.[11,17]

Furthermore, as the carboxyl content increased, the CNF suspension became more transparent, as observed by the light transmittance measurement shown in Figure 3. This result also indicated that the formation of homogenous nanofibers (finer fibrils) was obtained at a higher carboxyl content. In general, all characteristic behaviors of the CNFs and their suspension suggest that a greater surface charge of the CNF led to good dispersion of CNF in the PNIPAAm suspension, and will influence the microstructure of the CNF/PNIPAAm composite hydrogels.

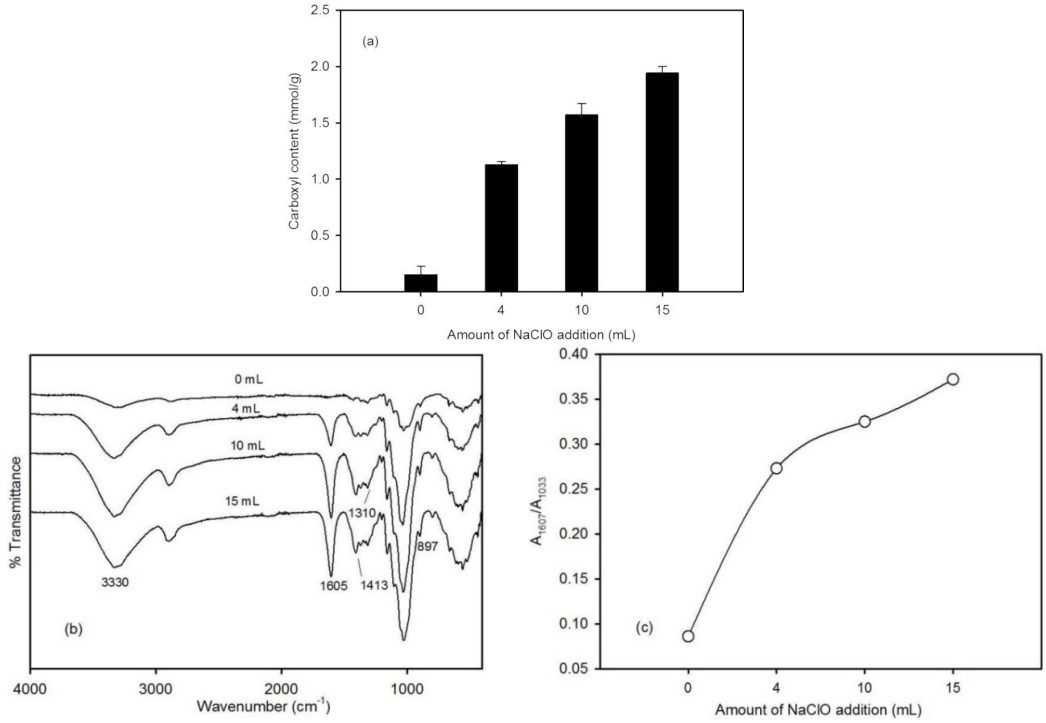

Figure 1: Characteristics of CNF isolated by TEMPO-mediated oxidation; (a) carboxylate content, (b) ATR-FTIR spectra, and (c) absorption ratio of A_{1607}/A_{1033} obtained from ATR-FTIR spectra

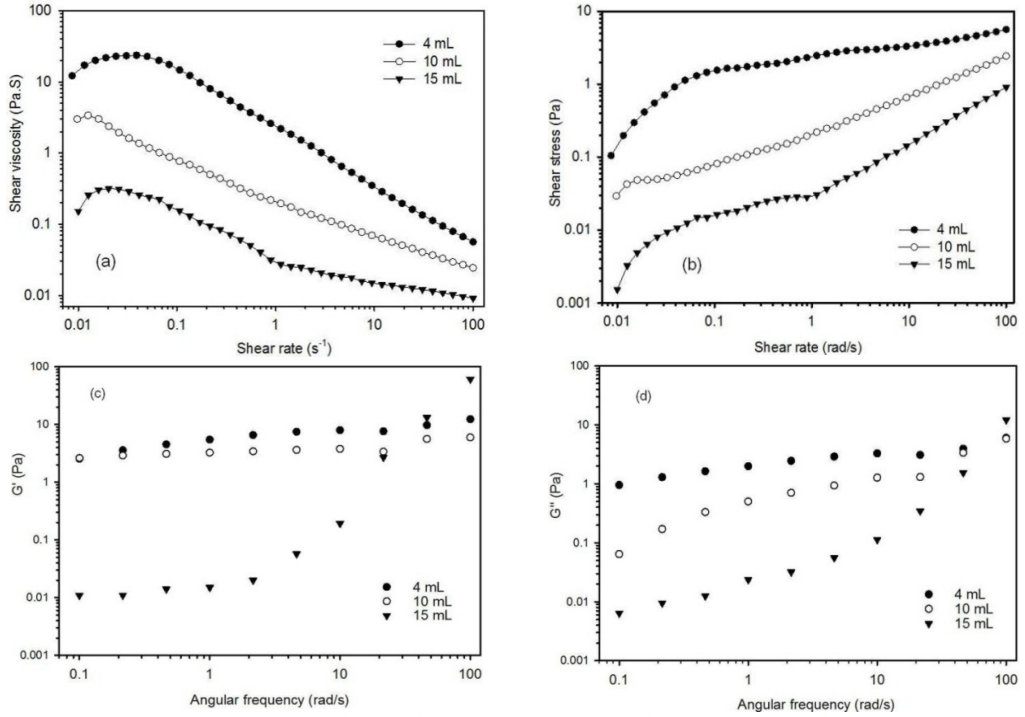

Figure 2: Rheological characteristics of CNF suspension at different amounts of NaClO; (a) shear viscosity, (b) shear stress, (c) storage modulus, and (d) loss modulus

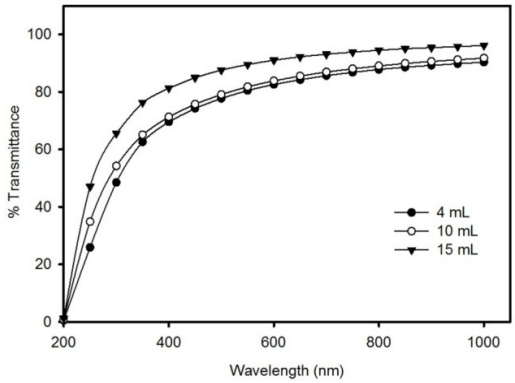

Figure 3: Transmittance of CNF suspensions at different amounts of NaClO using UV-Vis spectroscopy

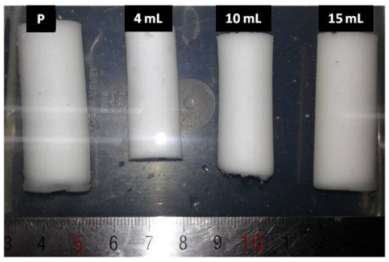

Figure 4: Image of pure PNIPAAm hydrogel (P) and CNF/PNIPAAm composite hydrogels at different addition levels of NaClO at room temperature and swollen state in water solution

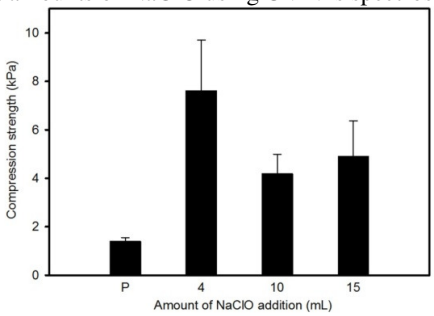

Figure 5: Compression strengths of pure PNIPAAm (P) and CNF/PNIPAAm composite hydrogels prepared with CNF at different addition levels of NaClO

Characterization of the CNF/PNIPAAm hydrogels

Morphology of composite hydrogels

Figure 4 exhibits images of pure PNIPAAm (P) and CNF/PNIPAAm composite hydrogels at different levels of carboxyl content. The images were obtained at room temperature in a water solution. All the hydrogels were swollen and opaque after the polymerization reaction was completed. There was no change in the translucency when the reaction was conducted at 70 °C, which was above the LCST of PNIPAAm (32 °C). Pure PNIPAAm and the composite hydrogels at 15 mL of NaClO had quite similar behaviors. However, different hydrogel characteristics were observed at 4 and 10 mL of NaClO. It can be seen from Figure 4 that in the equilibrium swelling state, the swelling of CNF-PNIPAAm at lower carboxyl content decreases dramatically, compared to that of pure PNIPAAm, although it slightly increases with an increase in the CNF surface charge.

At a lower carboxyl content, it caused a low dispersibility of the CNFs with a lower surface charge and caused poor dispersibility in the NIPAAm monomer suspension, which resulted in difficulties, such as low mixing ability, high gas entrapment, and high viscosity for the CNF/PNIPAAm composite hydrogels. However, as the surface charge increased, the dispersibility of CNFs in the NIPAAm solution improved, which made it easy to make the composite hydrogels for further characterization.

Compressive strength

Figure 5 shows the compressive strength of the CNF/PNIPAAm composite hydrogels at different carboxyl content. As expected, the introduction of CNFs into PNIPAAm clearly improved the compression strength of the composite hydrogels. This improvement suggested the successful stress load-transfer from the soft polymer to the stiff CNFs, owing to the reinforcement of CNFs.[9,10] However, the result is inconsistent with an increase in the carboxyl content. It is believed that CNFs with low carboxyl content or low surface charge form tight inter-connection networks *via* hydrogen bonds and entanglements of un-converted hydroxyl groups within fibrillated nanocellulose due to lower oxidant amount. These tight connections could have resulted in a stronger internal structure, leading to higher compressive

strength of the composite hydrogel. However, CNFs with high carboxyl content have a greater electrostatic repulsion and osmotic effect that could prevent the formation of hydrogen bonds between CNF, which consequently caused a decrease in the compressive strength. The CNF/-PNIPAAm composite hydrogel reinforced with CNF prepared at 10 mL NaClO had a lower compression strength and was weaker than the hydrogels prepared with CNFs and 15 mL NaClO. This might be caused by a difference in the CNF dispersion in the PNIPAAm matrix. In other words, the CNFs at the highest surface charge were homogenously dispersed in the PNIPAAm chains, leading to better reinforcement than those at 10 mL NaClO, even though greater oxidation resulted in a low level of hydrogen bonds in the composite hydrogels.[18] However, the compression strength of the composite hydrogels was relatively lower than that reported by Wei *et al*.[18] That could be attributed to the difference in the CNF loading in the composite hydrogel. We loaded 0.3% w/w CNF into the composite hydrogel, while they used 5% w/w in their hydrogels, which resulted in greater compression strength.

ATR FTIR spectroscopy

ATR-FTIR spectra of both PNIPAAm and CNF/PNIPAAm hydrogels with different amounts of carboxyl are shown in Figure 6. For the pure PNIPAAm polymer, the peaks at 1650 and 1540 cm^{-1} can be attributed to the-NH–C=O and N–H groups, respectively.[9] The FT-IR spectra of CNF/PNIPAAm hydrogels show that these two peaks become increasingly stronger and their intensity increased as the carboxyl content of the CNFs is increased. A broad absorption band at 3350 cm^{-1}could be due to the OH and NH stretching of the hydroxyl and amide groups of the CNF/PNIPAAm hydrogel. However, we did not find any peaks that are responsible for any chemical reaction between CNF and PNIPAAm. These results imply that the CNFs are just physically dispersed in the composite hydrogels.[9] Furthermore, other methods, like grafting of CNFs with an anionic surface charge *via* living radical polymerization (LRP), are necessary for chemical attaching CNFs into the PNIPAAm matrix[31,32] or grafting CNF with hydrophilic polyacrylamide prior to PNIPAAm.[33]

Lower critical solution temperature (LCST)

DSC measurements revealed an endothermic peak around 30°C for pure PNIPAAm and CNF/PNIPAAm composite hydrogels (Fig. 7). The endothermic peak temperature of the composite hydrogels did not change much as the carboxylate content increased. This fact indicated that the carboxylate content in CNF and the resultant surface charge level did not influence the balance between the hydrophilic and hydrophobic component on the polymer chains. In general, the LCST of the hydrogel decreases as the PNIPAAm chain contains more hydrophobic constituents.[34] However, the relatively constant LCST values obtained in this study could be due to several reasons. The first reason is the low content of CNF (*i.e*., 0.3 wt%) for the composite hydrogels.

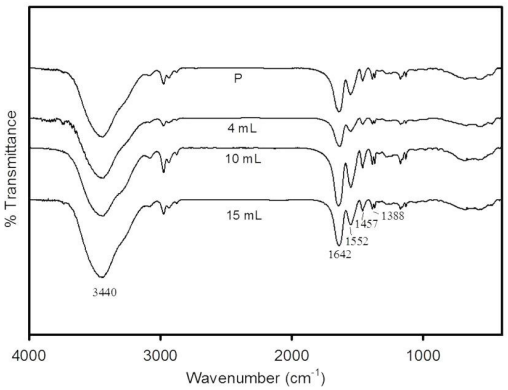

Figure 6: FT-IR spectra of PNIPAAm (P) and CNF-PNIPAAm hydrogels prepared with CNF at different addition levels of NaClO

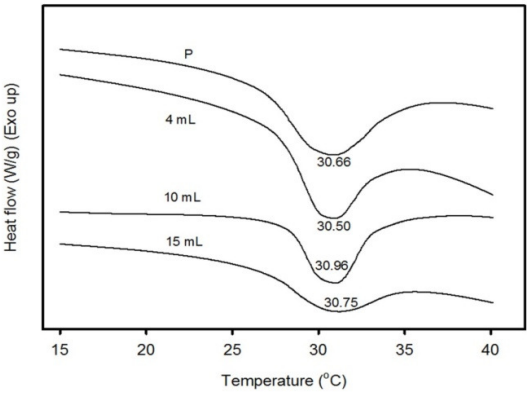

Figure 7: DSC thermograms of pure PNIPAAm and CNF/PNIPAAm composite hydrogels for determining their LCST as a function of the amount of added NaClO

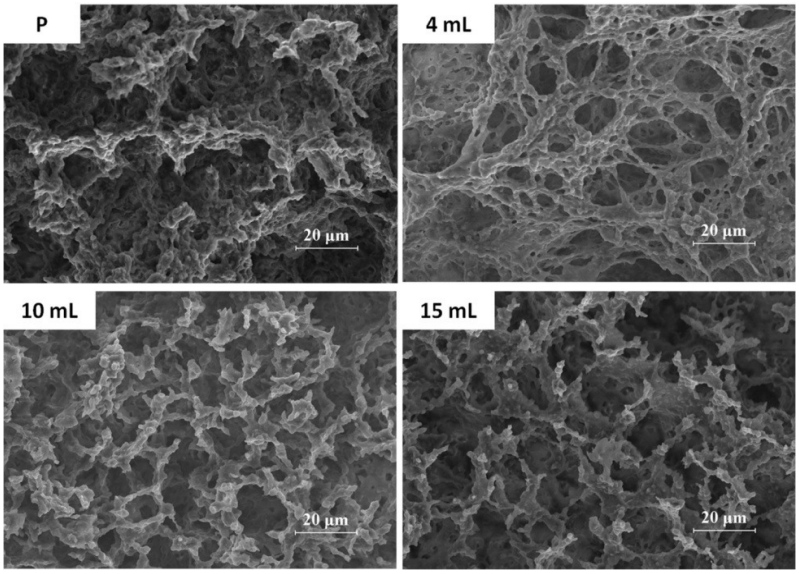

Figure 8: FE-SEM images of pure PNIPAAm and CNF-PNIPAAm hydrogels prepared with CNF at different addition levels of NaClO

Another reason is that there is no chemical interaction between CNF and PNIPAAm in the composite hydrogels as shown in Figure 6, because the presence of fully hydrophilic CNF constituents with surface charge resulted in no change in the LCST of the CNF/PNIPAAm composite hydrogels.[35]

Microscopic morphology

Microscopic images all hydrogels using FE-SEM are shown in Figure 8 in order to compare the internal morphology of the composite hydrogels at the same magnification level. All the hydrogel samples exhibited an irregular three-dimensional porous structure, but the CNF/PNIPAAm composite hydrogel that had been fabricated with CNFs isolated by adding 4 mL NaClO showed a homogenously interconnected fibril network structure. A long fibril network structure covered with the PNIPAAm matrix supported the entanglement of CNFs at lower carboxyl content, and provided an explanation for the greater compression strength, as shown in Figure 5. Different micro-morphologies were observed for the hydrogels prepared with CNFs isolated by adding 10 or 15 mL NaClO. CNFs were well dispersed in the PNIPAAm matrix. The morphology of pure PNIPAAm and the CNF/PNIPAAm hydrogels at 15 mL NaClO addition showed similar internal morphological structures.

Swelling behavior of hydrogels

Figure 9 shows the swelling behavior of all the hydrogels in distilled water. The swelling ratio of pure PNIPAAm hydrogels rapidly increased as the immersion time increased up to 100 min, followed by a relative constant swelling ratio thereafter. All the CNF/PNIPAAm hydrogels displayed a gradual increase in the swelling ratio, but the swelling ratios of the hydrogels were smaller than that of the pure polymer hydrogel. It is interesting to note that the addition of CNF into the PNIPAAm hydrogel does not improve its swelling ratio. This result contradicts the result reported by Cha *et al.*[9] This could be ascribed to the differences in the polymerization conditions and CNF loading. In addition, the physical entanglement between the PNIPAAm chains and CNF may cause an increase in the stiffness of the composite hydrogels, as explained in the compressive strength discussion, therefore it was compensated by the higher work needed to expand the network and consequently the CNF-PNIPAAm hydrogels were less swelled than that of pure PNIPAAm. However, regarding the carboxyl content in cellulose, the swelling ratio of the composite hydrogels increased as the carboxyl content of CNF increased. As the negatively charged carboxylate group increased, the electrostatic repulsion became dominant, which then facilitated the diffusion of water molecules into the network, contributing to the swelling of the hydrogel.

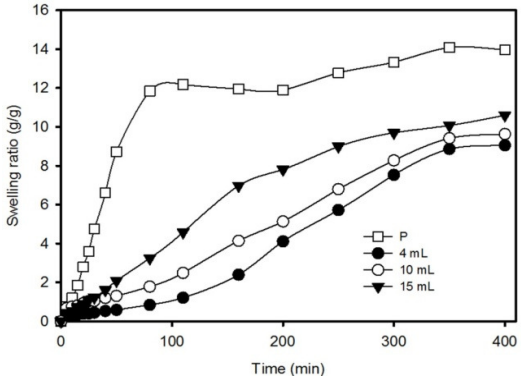

Figure 9: Swelling behavior of PNIPAAm and CNF-PNIPAAm hydrogels in distilled water

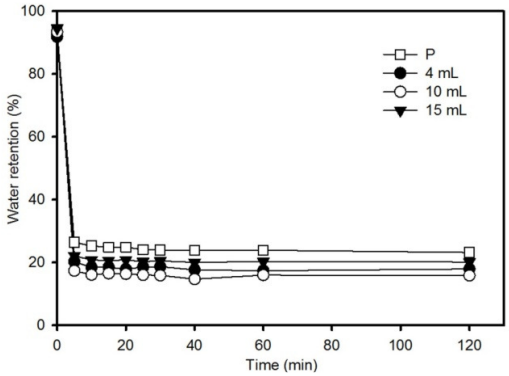

Figure 10: Water retention of PNIPAAm and CNF-PNIPAAm hydrogels prepared with CNF at different addition levels of NaClO

Water retention of hydrogels

The phase and volume transition of PNIPAAm above the LCST is an important characteristic of PNIPAAm-based hydrogels, which squeezes the water out of the hydrogels. Figure 10 exhibits the water retention changes of the PNIPAAm and CNF/PNIPAAM composite hydrogels at 50 °C, which is above the LCST. Although we expected the water to be released from the hydrogel above the LCST, both PNIPAAm and CNF/PNIPAAM hydrogels showed a very rapid decrease in the water retention, showing a fast response to temperature. Within five minutes (on the first measurement), the water released from pure PNIPAAm hydrogels reached around 75%, and then became constant, with no further changes. When CNFs with different levels of carboxylate were added, the CNF/PNIPAAm composite hydrogels showed a slight decrease in the water retention, indicating more release of water from the hydrogels. The lower water retention of the CNF/PNIPAAm composite hydrogels above the LCST could be due to their heterogeneous internal structure (microporous) that resulted from the polymerization above LCST[19] and the repulsive force of the CNF surface charge. This fast temperature response or fast deswelling of the composite hydrogels will be beneficial for developing functional hydrogels that show on-demand on-off switchable hydrogels.

CONCLUSION

This study reports on the development of various CNF/PNIPAAm composite hydrogels using CNFs with different carboxylate content, which were manipulated by adding different amounts of NaClO for TEMPO-mediated oxidation. First, we characterized the CNFs isolated by oxidation. As the carboxyl content increased, the shear viscosity and shear stress of the CNF suspension decreased, while the storage and loss modulus became more dependent on the angular frequency in the rheological measurements. As expected, the CNF surface charge increased with an increase in the amount of the oxidant, which resulted in a greater transparency owing to better CNF dispersion in the polymer suspension. The surface charge level of CNFs also influenced the compression strength of the CNF/PNIPAAm composite hydrogels. Specifically, a lower CNF surface charge level produced tight interconnections between the fibrils. The FT-IR spectra and the DSC results indicated that the CNFs were physically bonded onto the PNIPAAm in the hydrogels. These results showed that the CNF surface charge level had a great impact on the characteristics of the CNF/PNIPAAm hydrogels, indicating that the selection of a proper level of CNF surface charge and polymerization temperature is important for fast temperature-responsive hydrogels.

REFERENCES

[1] H. Fukuzumi, T. Saito, Y. Kumamoto, T. Iwata and A. Isogai, *Biomacromolecules*, **10**, 162 (2009).
[2] T. Saito and A. Isogai, *Ind. Eng. Chem. Res.*, **46**, 773 (2007).
[3] D. R. Paul and L. M. Robenson, *Polymer*, **49**, 3187 (2009).
[4] J. Nemoto, T. Soyama, T. Saito and A. Isogai, *Biomacromolecules*, **13**, 943 (2012).
[5] A. Azetsu, H. Koga, A. Isogai and T. Kitaoka, *Catalyst*, **1**, 83 (2011).
[6] F. Hoeng, A. Denneulin, C. Neuman and J. Bras, *J. Nanopart. Res.*, **17**, 244 (2015).

[7] N. Masruchin, B.-D. Park, V. Causin and I. C. Um, *Cellulose*, **22**, 1993 (2015).
[8] T. Saito, T. Uematsu, S. Kimura, T. Enomae and A. Isogai, *Soft Matter*, **7**, 8804 (2011).
[9] R. Cha, Z. He and Y.-H. Ni, *Carbohyd. Polym*., **88**, 713 (2012).
[10] J. Wei, Y. Chen, H. Liu, C. Du, H. Yu *et al*., *Carbohyd. Polym*., **147**, 201 (2016).
[11] A. Isogai, T. Saito and H. Fukuzumi, *Nanoscale*, **3**, 71 (2011).
[12] N. V. Ehman, Q. Tarres, M. Delgado-Aguilar, M. E.Vallejos, F. Felissia *et al*., *Cellulose Chem. Technol*., **50**, 361 (2016).
[13] A. Tejado, Md. N. Alam, M. Antal, H. Yang and T.G.M. van de Ven, *Cellulose*, **19**, 831 (2012).
[14] N. Masruchin and B.-D. Park, *J.Korean WoodSci. Technol*., **43**, 613 (2015).
[15] S. P. Mishra, J. Thirree, A.-S. Manent, B. Chabot and C. Daneault, *Bioresources*, **6**, 121 (2011).
[16] M. Xu, H.Q. Dai, X. Sun, S.M. Wang and W.B. Wu, *Bioresources*, **7**, 1633 (2012).
[17] L. Dai, Z. Long, Y. Lv and Q.-C. Feng, *Cellulose Chem. Technol*., **48**, 469 (2014).
[18] J. Wei, Y. Chen, H. Liu, C. Du, H. Yu*et al*., *Ind. Crop. Prod*., **92**, 227 (2016).
[19] G. Fundueanu, M. Constantin and P. Ascenzi, *Biomaterials*, **29**, 2767 (2008).
[20] X.-Z. Zhang, X.-D. Xu, S.-X. Cheng and R.-X. Zhuo, *Soft Matter*, **4**, 385 (2008).
[21] Z.-B. Hu, Y.-Y. Chen, C.-J. Wang, Y.-D. Zheng and Y. Li, *Nature*, **393**, 149 (1998).
[22] X.-D. Xu, H. Wei, X.-Z. Zhang, S.-X. Cheng and R.-X. Zhuo, *J. Biomed. Mater. Res. A*,**81**, 418 (2007).
[23] X.-F. Sun, H.-H. Wang, Z.-X. Jing and R. Mohanathas, *Carbohyd. Polym*., **92**, 1357 (2013).
[24] X. Z. Zhang and R. X. Zhuo, *J. Colloid. Interface Sci*., **223**, 311 (2000).
[25] X. Z. Zhang and R. X. Zhuo, *Eur. Polym. J*., **36**, 643 (2000).
[26] X. Z. Zhang and R. X. Zhuo, *Eur. Polym. J*., **36**, 2301 (2000).
[27] N. Masruchin, B.-D. Park and V. Causin, *J. Ind. Eng. Chem*., **29**,265 (2015).
[28] T. Saito, Y. Nishimura, J.-L. Putaux, M. Vignon and A. Isogai, *Biomacromolecules*, **7**, 1687 (2006).
[29] X.-F. Sun, Z. Gan, Z.-X. Jing, H.-H. Wang, D. Wang *et al*., *J. Appl. Polym. Sci*., **132**, 41606 (2015).
[30] E. Lasseuguette, *Cellulose*, **15**, 571 (2008).
[31] J. O. Zoppe, Y. Habibi,O. J. Rojas, R. A. Venditti, L.-S. Johansson *et al*., *Biomacromolecules*,**11**, 2683 (2010).
[32] U. D. Hemraz, A. Lu, R. Sunasee and Y. Boluk, *J. Colloid. Interface Sci*., **430**, 157 (2014).
[33] A. Hebeish, S. Farag, S. Sharaf and Th. I. Shaheen, *Int. J. Bio. Macromol*., **81**, 356 (2015).
[34] Y. Qiu and K. Park, *Adv. Drug Deliv. Rev*., **64**, 49 (2012).
[35] C. Alvarez-Lorenzo, A. Concheiro, A. S. Dubovik, N. V. Grinberg, T. V. Burova *et al*., *J. Control. Release*, **102**, 629 (2005).